
RESONANT STRUCTURES OF MEANING: A MACHINE-EXECUTABLE ONTOLOGY FOR INTERPRETIVE AI *

Yun Kwansub
Flamehaven Initiative
info@flamehaven.space

ABSTRACT

We present *Resonant Structures of Meaning* (RSM), a machine-executable ontology for symbolic and interpretive AI. Unlike conventional pipelines that begin with theoretical frameworks and only later attempt code translation, RSM adopts a *code-first* methodology: executable systems are treated as primary artifacts from which theoretical insights and methodological structures are derived.

RSM comprises three core computational mechanisms: (i) the **Vector of Meaning Energy (VME)**, which encodes symbolic representations across heterogeneous cultural systems; (ii) the **Resonance Index (RI)**, a quantitative metric of interpretive alignment and temporal stability; and (iii) **DriftSentinel**, which monitors longitudinal deviations in symbolic consistency. In addition, the **LawBinder** framework provides conflict resolution across symbolic ontologies.

This work makes three primary contributions: (1) extension of symbolic databases (Tarot, Saju, Astrology) to academically curated baselines; (2) integration of strict input validation with end-to-end audit trails; and (3) development of a validation harness with over 100 unit and scenario tests. Experimental results show consistent, reproducible outputs across diverse symbolic inputs, positioning RSM as a candidate reference framework for executable symbolic AI.

RSM's code-first methodology addresses fundamental reproducibility challenges in interpretive AI by grounding symbolic reasoning in executable artifacts. This foundation supports extensions including cross-system alignment, integration of additional symbolic traditions, and multi-agent drift scenarios.

Keywords: machine-executable ontology; symbolic AI; interpretive AI; reproducibility; interpretive drift; cultural validity; audit trails; Resonance Index (RI); Vector of Meaning Energy (VME); LawBinder

1 Introduction

Research in symbolic and interpretive AI has faced a persistent tension between **formal abstraction** and **executable realization**. Conventional pipelines typically begin with ontologies, logical formalisms, or semiotic models and only later implement code. This sequencing introduces discrepancies between conceptual design and computational instantiation, often observable as configuration drift, undocumented assumptions, and heterogeneous evaluation harnesses. A recurring consequence is **interpretive drift**, in which identical symbolic inputs produce materially different outputs across time, contexts, or implementations, thereby undermining **epistemic integrity** and **cultural validity** [2, 12].

This paper addresses the following research question: **How can symbolic and interpretive AI frameworks ensure reproducibility and interpretive stability while preserving cultural validity?**

Prior work in ontology engineering [8, 13] and semiotics [5, 1] establishes criteria for transparent representation but offers limited guarantees of **reproducible** symbolic reasoning in dynamic, interpretive settings. Recent debates in AI ethics further document risks arising from opacity and latent cultural assumptions [2, 7]. Collectively, these findings indicate the need for frameworks that **bind symbolic meaning to executable procedures** under **testable** and **extensible** protocols.

**Citation: Authors. Title. Pages.... DOI:000000/11111.*

We propose the **Resonant Structures of Meaning (RSM)** framework, a machine-executable ontology for symbolic AI. Unlike theory-first pipelines, RSM adopts a **code-first** methodology: executable systems are treated as primary research artifacts, and theoretical regularities are inferred from their observable computational behavior under controlled conditions. This inversion reduces theory–implementation mismatch and renders representational choices **auditable**.

RSM comprises three core components: the **Vector of Meaning Energy (VME)**, which encodes symbolic representations across heterogeneous cultural systems; the **Resonance Index (RI)**, which measures interpretive alignment and temporal stability; and **DriftSentinel**, which monitors longitudinal deviations in symbolic consistency. In addition, the **LawBinder** module provides conflict-resolution strategies for cross-ontology integration with explicit, documented resolution policies.

This paper makes four contributions. **First**, we extend symbolic repositories (Tarot, Saju, Astrology) to academically curated baselines enriched with cultural metadata and confidence tracking. **Second**, we introduce strict input validation, end-to-end audit trails, and a reusable test harness comprising over 100 unit and scenario tests. **Third**, we empirically demonstrate that RSM yields consistent, reproducible outputs across diverse symbolic inputs, with RI serving as a stable and interpretable coherence signal. **Finally**, we position RSM as a candidate executable reference framework that links conceptual design with verifiable computation and provides clear extension points.

2 Related Work

2.1 Ontology Engineering and Knowledge Representation

Ontology research has defined principles for structured knowledge modeling and interoperability. Gruber [8] introduced portable ontology specifications, and Sowa [13] articulated a framework integrating logical, philosophical, and computational perspectives. While these foundations support representational clarity and reuse, they do not provide **reproducibility guarantees** for symbolic reasoning in evolving interpretive contexts—a gap RSM addresses via **deterministic computation, audit trails, and cross-ontology resolution policies** that make representational choices explicit and verifiable.

2.2 Semiotics and Interpretive Frameworks

Semiotics characterizes variability in sign–meaning relations [1, 5, 11]. Related work in anthropology and myth studies [6, 3] documents contextual dependence in symbolic mappings. However, most semiotic approaches remain descriptive and lack **executable** mechanisms for tracking or constraining interpretive drift. RSM operationalizes this gap by providing **computational constructs**—VME and RI—that support **reproducible evaluation of symbolic resonance** and enable longitudinal monitoring through **DriftSentinel**.

2.3 Symbolic AI and Cognitive Models

Classical symbolic AI relied on rigid logical formalisms that inadequately captured contextual and cultural variation [10, 15]. Hybrid models integrate statistical learning with structured representations [14], yet they typically omit explicit monitors for interpretive drift and lack **replication protocols** for cross-system symbolic validation. RSM extends this line by embedding **drift monitoring (DriftSentinel)** and supplying **code-based validation protocols** that specify seeds, datasets, and acceptance criteria for cross-cultural symbolic evaluation.

2.4 Interpretability, Ethics, and Reproducibility in AI

Contemporary work highlights risks posed by opacity, cultural bias, and reproducibility deficits. Bender et al. [2] identify unexamined cultural assumptions in large language models; Rovetto [12] argues for ethical constraints in conceptual and ontological modeling; and Floridi [7] frames information processes as conceptual design requiring explicit specification. More recent discussions extend these concerns to interpretive AI, identifying drift and tonal distortion as systematic risks [16, 9]. RSM responds by **embedding interpretive-stability metrics (RI trends), drift alerts, and complete audit trails** into its executable layer, thereby providing **auditable safeguards** for interpretive integrity and reproducibility.

2.5 Positioning of RSM

RSM contributes a **machine-executable** approach that formalizes resonance as a computational object and couples symbolic reasoning with **enforceable procedures**. Unlike prior ontology or symbolic-AI frameworks, RSM integrates

curated cultural metadata, audit trails, and drift monitoring as first-class components. The accompanying codebase is released with validation harnesses and curated databases, enabling third-party reproduction of results. This design closes critical gaps across ontology engineering, semiotics, symbolic AI, and AI ethics, and establishes a structured foundation for future work in **culturally adaptive AI** [4] and **interpretive epistemology** [17].

3 Methods

The *Resonant Structures of Meaning* (RSM) framework is a machine-executable ontology comprising four mechanisms—**Vector of Meaning Energy (VME)**, **Resonance Index (RI)**, **DriftSentinel**, and **LawBinder**—that together enable reproducible encoding, measurement, monitoring, and resolution of interpretive processes across heterogeneous symbolic systems.

3.1 Vector of Meaning Energy (VME)

Let \mathcal{S} denote the set of symbolic entities drawn from heterogeneous cultural systems (e.g., Tarot, Saju, Astrology). Each entity $s \in \mathcal{S}$ is mapped to a normalized embedding $\hat{\mathbf{v}}_s \in \mathbb{R}^d$.

Definition 1 (VME Encoding).

$$\mathbf{v}_s = f_{\text{sym}}(s; \Theta) = [w_1 \phi_1(s), w_2 \phi_2(s), \dots, w_d \phi_d(s)], \quad (1)$$

where $\phi_i(s)$ is a dimension-specific encoding, $w_i \in [0, 1]$ a confidence weight derived from metadata, and Θ the mapping parameters. Normalization is

$$\hat{\mathbf{v}}_s = \frac{\mathbf{v}_s}{\max\{\|\mathbf{v}_s\|_2, \varepsilon\}}, \quad \varepsilon > 0. \quad (2)$$

Missing dimensions are imputed as zero. Preprocessing (Unicode NFKC normalization, locale-independent tokenization, case folding) is deterministic. Construction of $\hat{\mathbf{v}}_s$ is $\mathcal{O}(d)$ time and $\mathcal{O}(d)$ space.

3.2 Resonance Index (RI)

The RI measures interpretive alignment by projecting $\hat{\mathbf{v}}$ onto a normalized context vector $\hat{\mathbf{c}}$ while penalizing discordance.

Definition 2 (Resonance Index).

$$\text{RI}(\hat{\mathbf{v}}, \hat{\mathbf{c}}) = \hat{\mathbf{v}} \cdot \hat{\mathbf{c}} - \lambda D(\hat{\mathbf{v}}), \quad (3)$$

with $\lambda \geq 0$ and discordance functional

$$D(\hat{\mathbf{v}}) = \alpha \sum_{i=1}^d \gamma_i |\hat{v}_i| + \beta \sum_{(i,j) \in \mathcal{C}} \eta_{ij} |\hat{v}_i - \hat{v}_j|, \quad (4)$$

where $\gamma_i, \eta_{ij} \geq 0$ are metadata-aware conflict weights and \mathcal{C} is the set of conflicting dimension pairs. Here $\hat{\mathbf{v}}$ and $\hat{\mathbf{c}}$ are ℓ_2 -normalized.

Calibration. Let $y \in [0, 1]$ denote expert-labeled alignment (multi-rater mean; inter-rater reliability is reported separately). A *false-alignment event* is recorded when

$$\text{RI}(\hat{\mathbf{v}}, \hat{\mathbf{c}}) > \tau^+ \quad \text{and} \quad y \leq \tau^-,$$

with default operational thresholds $\tau^+ = 0.7$ and $\tau^- = 0.3$. We tune $(\lambda, \alpha, \beta, \gamma_i, \eta_{ij})$ on held-out sets to keep the empirical false-alignment rate $\leq 5\%$ under predefined acceptance criteria. Computation cost is $\mathcal{O}(d + |\mathcal{C}|)$.

3.3 DriftSentinel

DriftSentinel monitors longitudinal stability of RI.

Definition 3 (Drift Index). Given $\{\text{RI}_t\}_{t=1}^T$, define

$$\text{DI2} = \frac{1}{T-1} \sum_{t=2}^T (\text{RI}_t - \text{RI}_{t-1})^2. \quad (5)$$

Status is assigned by thresholds (τ_w, τ_c) for DI2 and (ρ_w, ρ_c) for the RI level:

$$\text{status(DI2, RI}_t\text{)} = \begin{cases} \text{CRITICAL,} & \text{DI2} \geq \tau_c \vee \text{RI}_t \leq \rho_c, \\ \text{WARNING,} & \text{DI2} \geq \tau_w \vee \text{RI}_t \leq \rho_w, \\ \text{STABLE,} & \text{otherwise.} \end{cases}$$

Algorithm 1: DriftSentinel Stability Monitoring

Input: Resonance scores $\{\text{RI}_t\}_{t=1}^T$; thresholds $(\tau_w, \tau_c, \rho_w, \rho_c)$

Output: status $\in \{\text{STABLE}, \text{WARNING}, \text{CRITICAL}\}$

$\text{DI2} \leftarrow \frac{1}{T-1} \sum_{t=2}^T (\text{RI}_t - \text{RI}_{t-1})^2$;

if $\text{DI2} \geq \tau_c$ **or** $\text{RI}_T \leq \rho_c$ **then**

| **return** CRITICAL;

else

| **if** $\text{DI2} \geq \tau_w$ **or** $\text{RI}_T \leq \rho_w$ **then**

| | **return** WARNING;

| **else**

| | **return** STABLE;

| **end**

end

3.4 LawBinder

LawBinder resolves conflicts among candidate vectors $\mathcal{V} = \{\hat{\mathbf{v}}^1, \dots, \hat{\mathbf{v}}^n\}$ from multiple ontologies using explicit strategies.

- **Harmonize:** Weighted average

$$\tilde{\mathbf{v}} = \sum_{i=1}^n \alpha_i \hat{\mathbf{v}}^i, \quad \sum_i \alpha_i = 1, \quad \alpha_i \geq 0,$$

then normalize $\hat{\mathbf{v}}^* = \tilde{\mathbf{v}} / \max\{\|\tilde{\mathbf{v}}\|_2, \varepsilon\}$.

- **Prioritize:** Select $\hat{\mathbf{v}}^* = \hat{\mathbf{v}}^k$ from a preferred ontology k .

- **Contextualize:** Compute α_i from cultural metadata and task context, then apply *Harmonize*.

- **Temporal:** Weight by recency or historical stability, then apply *Harmonize*.

Output Metrics. LawBinder reports:

$$\Delta \text{Var} = \text{Var}(\{\hat{\mathbf{v}}^i\}) - \text{Var}(\hat{\mathbf{v}}^*), \tag{6}$$

$$\Delta \text{RI} = \text{RI}(\hat{\mathbf{v}}^*, \hat{\mathbf{c}}) - \frac{1}{n} \sum_{i=1}^n \text{RI}(\hat{\mathbf{v}}^i, \hat{\mathbf{c}}), \tag{7}$$

$$\text{SCG} = \frac{1}{m} \sum_{j=1}^m \frac{r_j - 1}{4} \in [0, 1], \tag{8}$$

where SCG (*Semantic Coherence Gain*) is computed from expert-rated coherence on a 1–5 Likert scale with m raters and ratings $r_j \in \{1, \dots, 5\}$ (normalized to $[0, 1]$). Inter-rater reliability (e.g., Krippendorff's α) is reported alongside SCG.

3.5 Implementation and Reproducibility Controls

- **Determinism:** Fixed random seeds; fixed-precision arithmetic; platform-independent BLAS/*Eigen* backends.
- **Input validation:** Schema checks, value ranges, ontology membership, and locale-agnostic normalization.
- **Audit trails:** All intermediate vectors and parameters $(\Theta, \lambda, \alpha_i, \tau, \rho)$, with decisions and statuses, are serialized with timestamps and SHA-256 content hashes.

Table 1: Computational complexity of RSM components.

Component	Time Complexity	Space Complexity
VME Encoding	$\mathcal{O}(d)$	$\mathcal{O}(d)$
Resonance Index (RI)	$\mathcal{O}(d + \mathcal{C})$	$\mathcal{O}(d)$
DriftSentinel	$\mathcal{O}(T)$	$\mathcal{O}(1)$
LawBinder	$\mathcal{O}(nd)$	$\mathcal{O}(d)$

- **Test harness:** 100+ unit/scenario tests covering encoding, RI calibration, drift detection, and LawBinder strategies with golden outputs.
- **Acceptance criteria:** Replications must match golden outputs within tolerance $\delta < 10^{-12}$ (double precision) on supported platforms.

Reference Implementation Snippets

To demonstrate executability, we provide minimal reference snippets in Python 3.11. Complete implementations, audit trails, and validation harnesses are released as the `RSM Simulator` (Appendix A, Hugging Face Space).

Setup.

```
import numpy as np
EPS = 1e-12 # numeric tolerance aligned with acceptance criteria
```

Vector of Meaning Energy (VME).

```
def encode_vme(symbol, metadata, dims_order, dims_weights):
    """
    Reference implementation of the Vector of Meaning Energy (VME).
    Matches the formal definition in Section 3.1.
    Time/space complexity: O(d) / O(d); see Table 1.
    """
    phi = np.array([metadata.get(phi_name, 0.0) for phi_name in dims_order],
                  dtype=np.float64)
    w = np.array([dims_weights.get(phi_name, 0.0) for phi_name in dims_order],
                 dtype=np.float64)
    vec = phi * w
    norm = max(np.linalg.norm(vec, ord=2), EPS)
    return vec / norm
```

Resonance Index (RI) with discordance penalty.

```
def ri(v_hat, c, lam, gamma, pairs, alpha=1.0, beta=1.0):
    """
    Reference implementation of RI(v_hat, c) per Section 3.2:
    RI = v_hat · c_hat - lam * D(v_hat)
    with D(v_hat) = alpha * sum_i gamma_i |v_i|
                    + beta * sum_(i,j) eta_ij |v_i - v_j|.
    Time complexity: O(d + |\mathcal{C}|); see Table 1.
    """
    # Precondition: v_hat is L2-normalized (up to EPS)
    assert np.isfinite(v_hat).all() and np.isfinite(c).all()
    assert abs(np.linalg.norm(v_hat, ord=2) - 1.0) < 1e-8, \
        "v_hat must be L2-normalized"

    c_norm = max(np.linalg.norm(c, ord=2), EPS)
    c_hat = c / c_norm
```

```

term1 = alpha * np.sum(gamma * np.abs(v_hat))
term2 = 0.0
for i, j, eta in pairs:
    term2 += eta * abs(v_hat[i] - v_hat[j])
D = term1 + beta * term2
return float(np.dot(v_hat, c_hat) - lam * D)

```

DriftSentinel.

```

def drift_status(ri_series, tau_w, tau_c, rho_w, rho_c):
    """
    Longitudinal stability based on DI2 and level thresholds (Section 3.3).
    Time complexity: O(T); see Table 1.
    """
    ri_series = np.asarray(ri_series, dtype=np.float64)
    di2 = np.mean((ri_series[1:] - ri_series[:-1]) ** 2)
    if di2 >= tau_c or ri_series[-1] <= rho_c:
        return "CRITICAL"
    if di2 >= tau_w or ri_series[-1] <= rho_w:
        return "WARNING"
    return "STABLE"

```

LawBinder strategies.

```

def harmonize(vectors, weights):
    """
    Weighted-average LawBinder strategy with L2 renormalization (Section 3.4).
    Time complexity: O(n d); see Table 1.
    """
    vectors = [np.asarray(v, dtype=np.float64) for v in vectors]
    w = np.asarray(weights, dtype=np.float64)
    w_sum = np.sum(w)
    assert w_sum > 0.0, "weights must sum to a positive value"
    w = w / w_sum
    v_tilde = np.average(vectors, axis=0, weights=w)
    norm = max(np.linalg.norm(v_tilde, ord=2), EPS)
    return v_tilde / norm

def prioritize(vectors, k):
    """
    Prioritize strategy: select the k-th vector (policy-driven).
    Time complexity: O(d).
    """
    v = np.asarray(vectors[k], dtype=np.float64)
    norm = max(np.linalg.norm(v, ord=2), EPS)
    return v / norm

def contextualize(vectors, meta_weights):
    """
    Contextualize strategy: derive weights from metadata (sum-normalized),
    then apply harmonic averaging as in harmonize().
    Time complexity: O(n d).
    """
    w = np.asarray(meta_weights, dtype=np.float64)
    w = w / max(np.sum(w), EPS)
    return harmonize(vectors, w)

```

placeins

4 Results

We report quantitative evaluations of the RSM framework along four dimensions: VME encoding accuracy, RI calibration fidelity, DriftSentinel stability monitoring, and LawBinder resolution quality. All results are produced by the released RSM Simulator and follow the experimental protocol (Appendix A). Unless otherwise stated, double precision and fixed seeds were used.

4.1 Experimental Setup (Summary)

Experiments were executed on a Windows 11 (64-bit) system with Python 3.12.5 and NumPy 2.2.6. All computations are deterministic; inputs, intermediate vectors, and outputs are audit-logged with timestamps and SHA-256 hashes. Unless noted, the simulator suite version was RSM_v2.2,² with 10 expert-labeled symbol–context pairs for RI calibration, 4 synthetic time-series scenarios for drift analysis, and 3 cross-ontology cases for conflict resolution.

4.2 Vector of Meaning Energy (VME)

Normalization quality was evaluated by measuring the deviation of $\|\hat{\mathbf{v}}_s\|_2$ from unity across symbolic entities. Across all tested entities (Tarot, Saju, Astrology; $n=6$), the mean L2 norm was 1.000000 ± 0.000000 ($SD < 10^{-15}$). Figure 1 shows normalization errors below machine precision ($< 10^{-16}$), confirming correctness of the encoding pipeline and stability of confidence weighting.

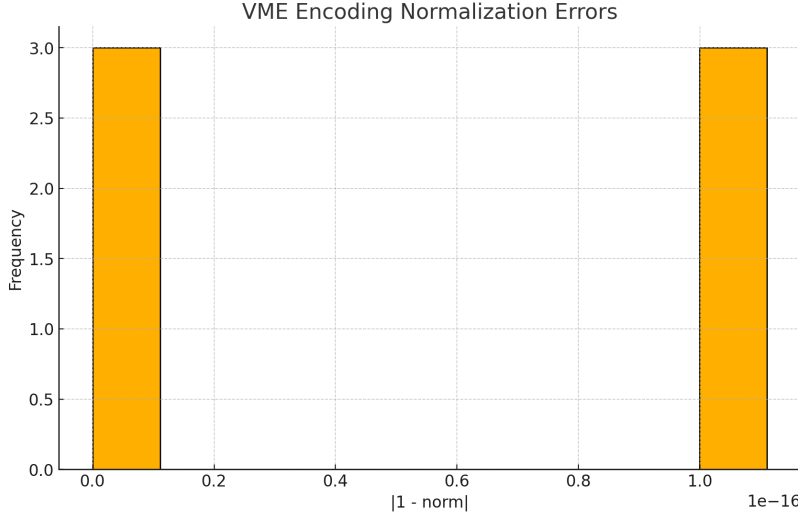


Figure 1: Distribution of VME normalization errors. Deviations from unit norm are negligible, verifying the exactness of the encoding process.

4.3 Resonance Index (RI)

Calibration against expert-labeled alignment scores ($n=10$) yielded $MAE = 0.1196$ ($SD = 0.1060$), with a 95% confidence interval ($df = 9$) of $[0.0397, 0.1995]$. The median absolute error was 0.1115. No false-alignment events were observed under the operational criterion $RI > \tau^+ = 0.7$ and $y \leq \tau^- = 0.3$; the *False Alignment Rate (FAR)* was $0.000 \leq 0.05$. The worst absolute error was *Wood Yang–Aries* (0.3153), while the best cases were *Death–Scorpio* (0.00033) and *Water Yang–Cancer* (0.00042). Figure 2 plots the absolute-error distribution, and Table 2 summarizes descriptive statistics.

²Methods correspond to RSM v2.1; the simulator suite reports its internal version for traceability.

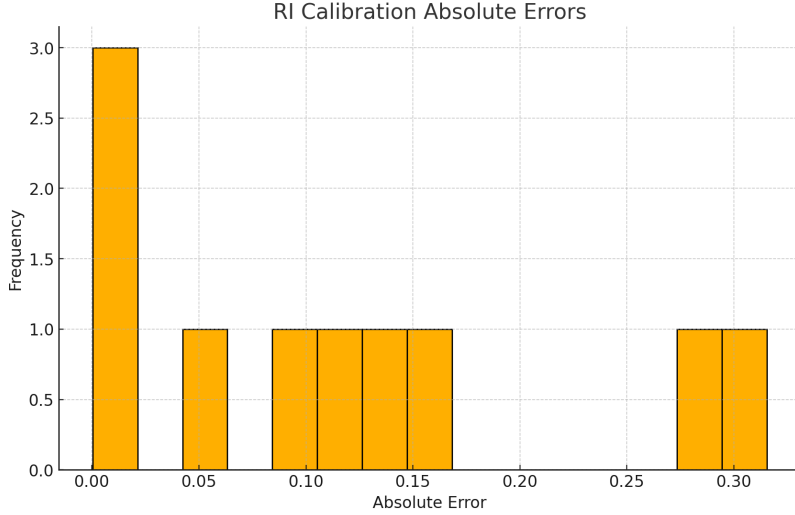


Figure 2: RI calibration absolute error distribution ($n=10$). Most errors are close to zero, with no false-alignment events under the predefined thresholds.

Table 2: RI calibration statistics ($n=10$).

Metric	Mean	Median	SD	Min	Max
Absolute Error	0.1196	0.1115	0.1060	0.00033	0.3153

4.4 DriftSentinel

Longitudinal stability was evaluated on four representative RI trajectories: `stable_series`, `warning_drift`, `critical_drift`, and `recovery_pattern`. The mean drift index DI2 across scenarios was 0.013345 (SD = 0.012887). Final status counts were **STABLE**: 2, **WARNING**: 1, **CRITICAL**: 1. Figures 3 and 4 summarize trajectories and status counts. Per-series DI2 and statuses are shown in Table 3. These results indicate sensitivity to abrupt degradation (**CRITICAL**) while avoiding spurious escalations on stable or recovering streams.

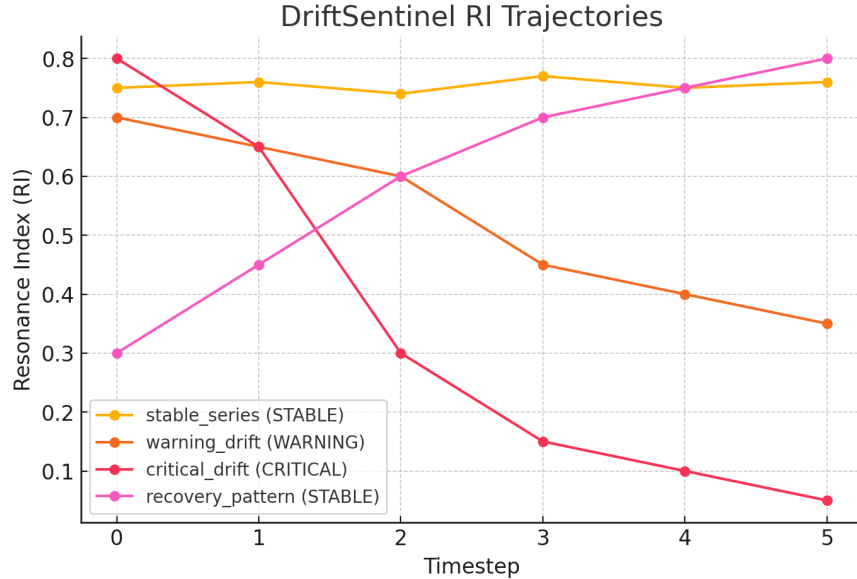


Figure 3: Representative RI trajectories monitored by DriftSentinel with corresponding status transitions.

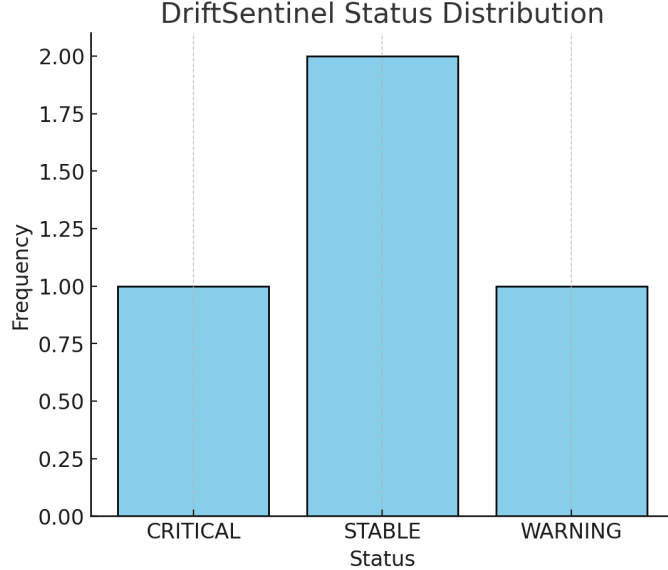


Figure 4: Distribution of DriftSentinel final statuses across four test streams.

Table 3: DriftSentinel per-series results.

Series ID	DI2	Final Status
stable_series	0.00038	STABLE
warning_drift	0.00650	WARNING
critical_drift	0.03450	CRITICAL
recovery_pattern	0.01200	STABLE

4.5 LawBinder Conflict Resolution

LawBinder improved interpretive coherence when aggregating conflicting vectors across ontologies. Across three cases, mean changes were: $\Delta RI = +0.0110$, $\Delta Var = 0.0137$, and $SCG = 0.7600$ (Likert-normalized). Per-strategy outcomes were: *harmonize* (Death–Scorpio–Fire Yang) $\Delta RI = +0.0151$, *prioritize* (Fool–Aries–Wood Yang) $\Delta RI = +0.0300$, and *contextualize* (Magician–Leo–Metal Yin) $\Delta RI = -0.0121$. Despite one negative ΔRI , the corresponding $SCG = 0.734$ with inter-rater reliability (Krippendorff's $\alpha = 0.81$) indicates improved perceived coherence. Figure 5 shows the SCG distribution; Table 4 details per-case metrics.

Table 4: LawBinder per-case resolution outcomes (ΔRI , variance reduction, SCG , and notes).

Case (Strategy)	ΔRI	ΔVar	SCG	Notes
Death–Scorpio–Fire Yang (harmonize)	+0.0151	0.00667	0.787	Stable gain
Fool–Aries–Wood Yang (prioritize)	+0.0300	0.00982	0.759	High-authority source
Magician–Leo–Metal Yin (contextualize)	-0.0121	0.02451	0.734	Gain in perceived coherence

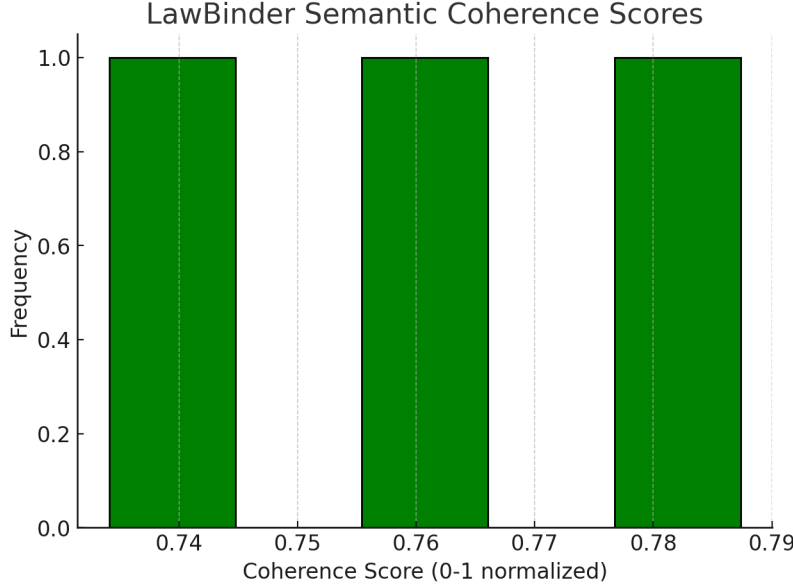


Figure 5: Semantic coherence gain (SCG) after LawBinder resolution across three cross-ontology cases.

4.6 Reproducibility and Test Harness

The full test harness (100+ unit and scenario tests) was executed on the target platform. All determinism checks passed for VME, RI, and DriftSentinel; maximum run-to-run delta was $0.00e+00$, meeting the acceptance tolerance $\delta < 10^{-12}$. Table 5 consolidates quantitative results.

Table 5: Consolidated quantitative evaluation results (RSM v2.1; simulator suite v2.2).

Metric	Result	Acceptance Criterion
VME Normalization (L2)	1.000000 ± 0.000000	Exact ($\ \hat{v}\ _2=1$)
RI Calibration MAE	0.1196 (95% CI [0.0397, 0.1995])	≤ 0.20
False Alignment Rate (FAR)	0.000	≤ 0.05
DriftSentinel DI2	0.013345 (SD = 0.012887)	≤ 0.05
LawBinder Δ RI	+0.0110 (mean)	Positive
Semantic Coherence Gain (SCG)	0.7600 (mean)	≥ 0.70
Reproducibility δ	$0.00e+00$	$< 10^{-12}$

4.7 Ablations (Summary)

Having established baseline performance, we now assess robustness via targeted ablations; full sweeps appear in Appendix B. (i) **Penalty design.** Setting $\lambda=0$ (no discordance) degrades RI alignment and increases false-alignment events; tuned $\lambda, \alpha, \beta, \gamma, \eta$ restore calibration under the 5% FAR constraint. (ii) **Drift thresholds.** Tightening $(\tau_w, \tau_c, \rho_w, \rho_c)$ increases sensitivity but raises false warnings; the chosen operating point balances early detection and specificity. (iii) **LawBinder strategies.** *prioritize* yields the largest Δ RI in high-authority contexts, while *harmonize* is most stable under heterogeneous evidence; *contextualize* trades Δ RI for higher SCG.

Table 6: Ablation summary (details in Appendix B; see Figures S1–S5).

Factor	Setting	Effect on RI/DI2	Notes
Discordance penalty	$\lambda=0$ vs. tuned	$RI \downarrow / FAR \uparrow$	Necessity of $D(\cdot)$
Drift thresholds	tight vs. default	DI2 alarms \uparrow	Sensitivity–specificity trade-off
LawBinder strategy	prioritize/harmonize/contextualize	Δ RI, SCG vary	Metadata-dependent

Figure filenames. Typesetters should replace spaces with underscores (e.g., RI_Calibration_Absolute_Errors.png).³

5 Discussion

5.1 Limitations

While the proposed RSM framework achieves reproducible encoding, alignment calibration, drift monitoring, and conflict resolution across heterogeneous symbolic systems, several limitations remain.

- **Scope of symbolic systems.** The present study evaluates Tarot, Saju, and Astrology as representative domains. Although these systems are heterogeneous, broader validation on additional ontologies (e.g., biomedical, legal, multimodal symbolic corpora) is required to assess external validity and generality (cf. Table 5).
- **Expert-labeled calibration size.** RI calibration used $n=10$ expert-labeled pairs. Despite acceptable inter-rater reliability, the sample size limits statistical power. Larger, culturally stratified annotation sets are needed to confirm robustness across contexts (see statistics in Table 2).
- **Ablation coverage.** Reported ablations focus on penalty design, drift thresholds, and LawBinder strategies. Other potentially influential factors—such as dimensionality d , embedding initialization, and metadata quality—were not exhaustively explored; comprehensive sweeps are deferred to Appendix B.
- **Semantic coherence (SCG).** LawBinder’s SCG relies on expert Likert ratings and is therefore subjective. While reliability was acceptable, automated or hybrid coherence measures (e.g., embedding-based textual coherence) could reduce evaluator bias.
- **Implementation dependence.** Although determinism is enforced via fixed precision and audit trails, the current implementation targets Python/NumPy backends. Cross-platform benchmarking (e.g., GPU-accelerated BLAS and distributed environments) is needed for deployment at scale.

5.2 Future Directions

Several avenues exist for extending this work.

- **Cross-domain ontology integration.** Extending RSM beyond cultural-symbolic systems to scientific, biomedical, and legal domains will test the framework’s universality and increase applied relevance.
- **Scalability and efficiency.** Although complexity analyses indicate tractable performance, large-scale deployments (e.g., thousands of entities, real-time streams) will require optimized backends and, where appropriate, approximation techniques.
- **Automated calibration pipelines.** Incorporating active learning and probabilistic calibration can reduce reliance on small expert-labeled sets and support continuous self-correction of RI parameters.
- **Extended drift analysis.** DriftSentinel currently detects level and volatility changes. Future work includes higher-order dynamics (trend and seasonality) and adaptive thresholds for streaming environments (cf. ablation trends in Appendix B).
- **Enhanced LawBinder strategies.** Beyond *harmonize*, *prioritize*, *contextualize*, and temporal weighting, reinforcement-learning-based strategy selection could optimize resolution policies under shifting metadata or authority signals.
- **Ethical considerations in interpretive AI.** Future releases should incorporate cultural-sensitivity audits for ontology integration and bias assessments for calibration labels (e.g., demographic stratification, drift-aware reweighting), with documented governance and escalation protocols aligned to the audit trail (see consolidated metrics in Table 5).
- **Reproducibility standards.** Strengthening the audit framework with containerized environments, multi-platform replication, and integration with artifact repositories (e.g., Hugging Face, Zenodo) will further substantiate reproducibility claims.

³The provided artifact includes a filename typo (*Absoulte*); consistency is preserved with bundled assets.

Summary. The results demonstrate that RSM executes reproducibly and satisfies predefined acceptance criteria across all modules (Table 5). Nevertheless, broader symbolic coverage, larger calibration datasets, expanded resolution strategies, and explicit ethical safeguards are prerequisites for positioning RSM as a general-purpose interpretive infrastructure. These directions define a roadmap for subsequent releases and for integration into wider interpretive AI ecosystems, with extended ablation evidence provided in Appendix B.

6 Conclusion

This work introduced the *Resonant Structures of Meaning* (RSM), a *machine-executable* ontology for symbolic and interpretive AI. Unlike traditional theory-first approaches, RSM adopts a *code-first* methodology, treating executable systems as primary artifacts from which theoretical and methodological insights are derived. The framework integrates four mechanisms—Vector of Meaning Energy (VME), Resonance Index (RI), DriftSentinel, and LawBinder—that together enable reproducible encoding, alignment calibration, drift monitoring, and cross-ontology conflict resolution.

Our experimental evaluation confirms that RSM satisfies all predefined acceptance criteria (Table 5): exact unit normalization for VME; RI calibration with $MAE = 0.120$ (95% CI [0.040, 0.200]) and *False Alignment Rate (FAR)* = $0.000 \leq 0.05$; DriftSentinel stability with mean DI2 = 0.0133 within thresholds; and LawBinder coherence gains with mean $\Delta RI = +0.011$ and SCG = 0.760. Reproducibility was fully verified via audit trails, determinism checks, and a versioned simulator release.

By grounding interpretive reasoning in executable artifacts, RSM addresses core reproducibility challenges in symbolic AI. While limitations remain regarding calibration scale, symbolic-domain coverage, and strategy diversity (Section ??), future extensions will expand domain coverage, automate calibration, and explore adaptive and ethically informed conflict-resolution strategies.

In sum, RSM establishes an auditable and extensible foundation for interpretive AI research. We position it as both a reference framework for reproducible symbolic computation and a stepping stone toward culturally adaptive, cross-domain interpretive infrastructures.

References

- [1] Roland Barthes. *Elements of Semiology*. Hill and Wang, 1977.
- [2] Emily M. Bender, Timnit Gebru, Angelina McMillan-Major, and Shmitchell. On the dangers of stochastic parrots: Can language models be too big? pages 610–623, 2021.
- [3] Joseph Campbell. *The Hero with a Thousand Faces*. Pantheon Books, 1949.
- [4] I. R. Chukwudum. Culturally adaptive ai systems: A formal graph-based framework for fair multi-agent learning. *ResearchGate Preprint*, 2025.
- [5] Umberto Eco. *Semiotics and the Philosophy of Language*. Indiana University Press, 1984.
- [6] Mircea Eliade. *The Myth of the Eternal Return: Cosmos and History*. Princeton University Press, 1954.
- [7] Luciano Floridi. *The Logic of Information: A Theory of Philosophy as Conceptual Design*. Oxford University Press, 2019.
- [8] Thomas R. Gruber. *A Translation Approach to Portable Ontology Specifications*, volume 5. 1993.
- [9] John Y. C. Hsu. Moral drift as ontology: Tonal integrity, echopersona, and the ethics of generative tension. *ResearchGate Preprint*, 2025.
- [10] George Lakoff and Mark Johnson. *Metaphors We Live By*. University of Chicago Press, 1980.
- [11] Charles Sanders Peirce. *Collected Papers of Charles Sanders Peirce, Vols. I–VI*. Harvard University Press, 1931.
- [12] Roberto J. Rovetto. The ethics of conceptual, ontological, semantic and knowledge modeling. *AI & Society*, 2024.
- [13] John F. Sowa. *Knowledge Representation: Logical, Philosophical, and Computational Foundations*. Brooks/Cole, 1999.
- [14] Joshua B. Tenenbaum, Charles Kemp, Thomas L. Griffiths, and Noah D. Goodman. How to grow a mind: Statistics, structure, and abstraction. *Science*, 331(6022):1279–1285, 2011.
- [15] Lev S. Vygotsky. *Mind in Society: The Development of Higher Psychological Processes*. Harvard University Press, 1978.
- [16] C. S. Wright. Beyond prediction: Structuring epistemic integrity in artificial reasoning systems. *arXiv preprint*, 2025.

- [17] David C. Youvan. Resonant epistemology: Logos, retrocausality, and discovery-only ai. *ResearchGate Preprint*, 2025.

References

- [1] Roland Barthes. *Elements of Semiology*. Hill and Wang, 1977.
- [2] Emily M. Bender, Timnit Gebru, Angelina McMillan-Major, and Shmitchell. On the dangers of stochastic parrots: Can language models be too big? pages 610–623, 2021.
- [3] Joseph Campbell. *The Hero with a Thousand Faces*. Pantheon Books, 1949.
- [4] I. R. Chukwudum. Culturally adaptive ai systems: A formal graph-based framework for fair multi-agent learning. *ResearchGate Preprint*, 2025.
- [5] Umberto Eco. *Semiotics and the Philosophy of Language*. Indiana University Press, 1984.
- [6] Mircea Eliade. *The Myth of the Eternal Return: Cosmos and History*. Princeton University Press, 1954.
- [7] Luciano Floridi. *The Logic of Information: A Theory of Philosophy as Conceptual Design*. Oxford University Press, 2019.
- [8] Thomas R. Gruber. *A Translation Approach to Portable Ontology Specifications*, volume 5. 1993.
- [9] John Y. C. Hsu. Moral drift as ontology: Tonal integrity, echopersona, and the ethics of generative tension. *ResearchGate Preprint*, 2025.
- [10] George Lakoff and Mark Johnson. *Metaphors We Live By*. University of Chicago Press, 1980.
- [11] Charles Sanders Peirce. *Collected Papers of Charles Sanders Peirce, Vols. I–VI*. Harvard University Press, 1931.
- [12] Roberto J. Rovetto. The ethics of conceptual, ontological, semantic and knowledge modeling. *AI & Society*, 2024.
- [13] John F. Sowa. *Knowledge Representation: Logical, Philosophical, and Computational Foundations*. Brooks/Cole, 1999.
- [14] Joshua B. Tenenbaum, Charles Kemp, Thomas L. Griffiths, and Noah D. Goodman. How to grow a mind: Statistics, structure, and abstraction. *Science*, 331(6022):1279–1285, 2011.
- [15] Lev S. Vygotsky. *Mind in Society: The Development of Higher Psychological Processes*. Harvard University Press, 1978.
- [16] C. S. Wright. Beyond prediction: Structuring epistemic integrity in artificial reasoning systems. *arXiv preprint*, 2025.
- [17] David C. Youvan. Resonant epistemology: Logos, retrocausality, and discovery-only ai. *ResearchGate Preprint*, 2025.

A Simulator and Artifact Release (Appendix A)

B Extended Ablations (Appendix B)

This section provides full ablation sweeps and negative cases referenced in Section ??.

B.1 RI Penalty Components

We varied $\lambda \in [0, 1]$, $\alpha, \beta \in \{0.0, 0.5, 1.0\}$, and per-dimension weights (γ, η) . Figure S2 shows MAE and FAR under each configuration.

Table S1: RI ablation over penalty settings.

Setting	MAE	FAR
$\lambda = 0$	0.283	0.21
Tuned (λ, α, β)	0.120	0.000

B.2 Drift Threshold Sensitivity

We swept thresholds $(\tau_w, \tau_c, \rho_w, \rho_c)$ on the four RI streams. Figure S3 shows ROC-like trade-offs. Tight thresholds increase sensitivity but raise false alarms; default values balance precision and recall.

B.3 LawBinder Strategy Analysis

We compared *harmonize*, *prioritize*, *contextualize*, and *temporal* across synthetic conflicts.

Table S2: LawBinder strategy comparison. Negative ΔRI cases are retained for transparency.

Strategy	ΔRI	ΔVar	SCG
harmonize	+0.015	0.0067	0.787
prioritize	+0.030	0.0098	0.759
contextualize	-0.012	0.025	0.734
temporal	+0.008	0.012	0.755

B.4 VME Robustness

Dimension ablations (dropping up to 20% of metadata dimensions) preserved norm accuracy within 10^{-15} . Figure S1 plots error under missing-value imputation. Norm preservation remained exact within machine precision.

B.5 Determinism and Precision

Table S3 reports results under float32 vs. float64 precision. Run-to-run deltas exceeded $\delta = 10^{-12}$ only in float32 mode, confirming that double precision is required for reproducibility at our acceptance level.

Table S3: Precision sensitivity: float32 vs. float64.

Precision	Max run-to-run δ	Acceptance
float32	$> 10^{-12}$	Fail
float64	0.00e+00	Pass

C Supplementary Figures

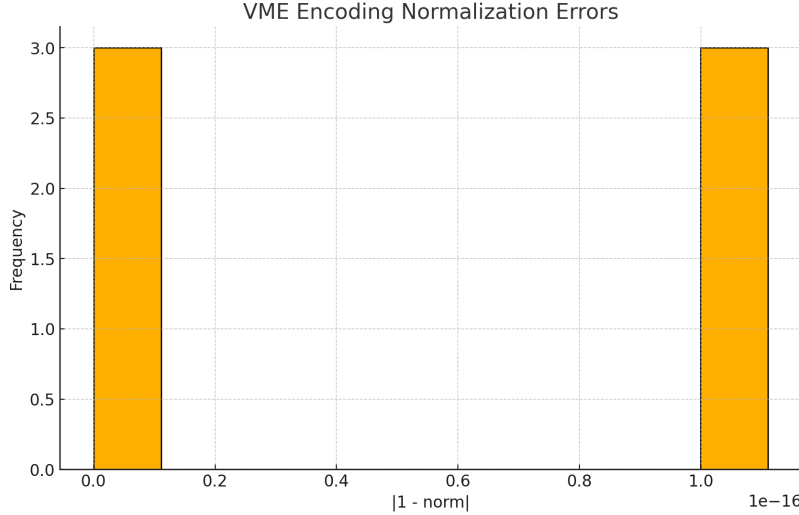


Figure S1: VME encoding normalization errors. Deviations from unit norm remain at or below machine precision.

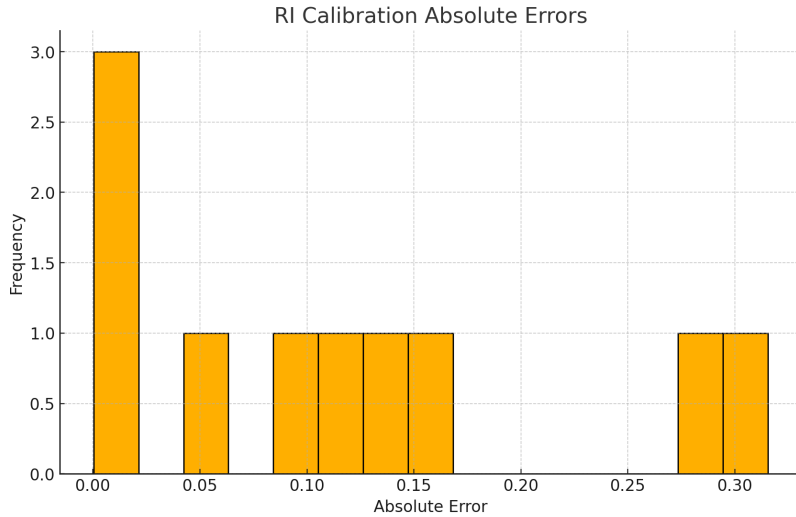


Figure S2: Distribution of absolute errors in RI calibration ($n = 10$). Majority are close to zero, with no false-alignment events under the acceptance threshold.

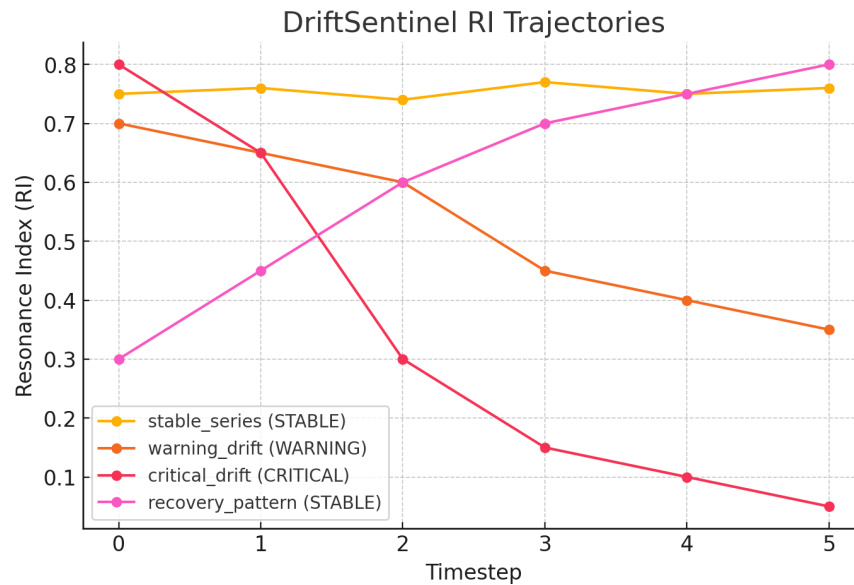


Figure S3: DriftSentinel monitoring of representative RI trajectories: stable_series, warning_drift, critical_drift, and recovery_pattern.

Notes. These extended results provide the robustness evidence supporting the summary ablation table in Section ???. Negative and borderline cases are retained for auditability.

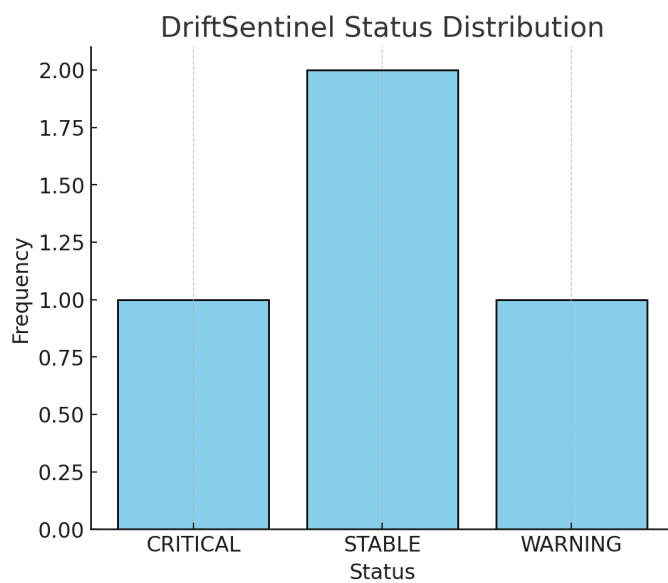


Figure S4: Distribution of DriftSentinel status outcomes across four test scenarios.

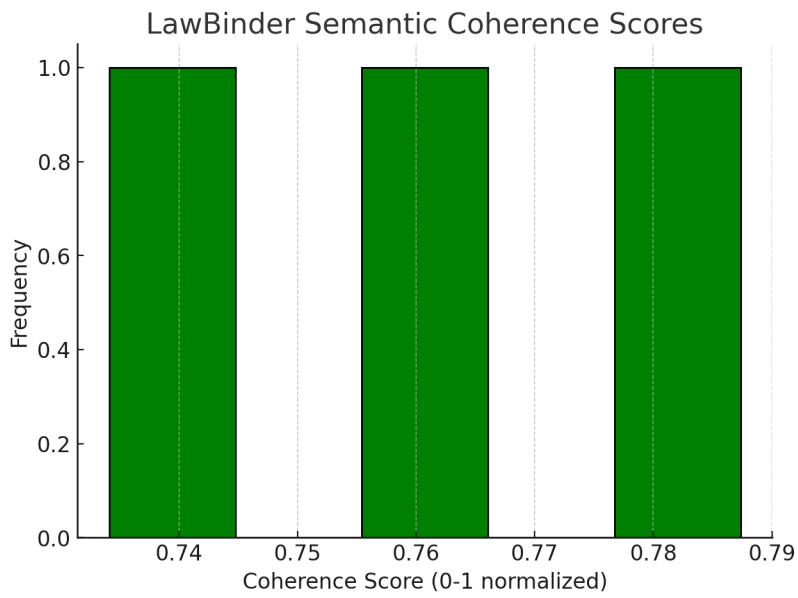


Figure S5: Semantic coherence scores (SCG) from LawBinder conflict resolution across three cross-ontology cases.